Proceedings of the XII International Symposium on Dynamic Problems of Mechanics (DINAME 2007),
Varoto, P. S. and Trindade, M. A. (Editors), ABCM, Ilhabela, SP, Brazil, February 26 - March 2, 2007

Mechanical Fault Diagnosis in a Flexible Rotor through Correlations Functions and Artificial Neural Network

Gilberto Machado da Silva [1], Robson Pederiva [2]

[1] Tecnological Center of Brazilian Navy – Av. Prof Lineu Prestes, 2242 - Zip Code: 05598-000- São Paulo - SP- Brasil, Fax: 55-11-38144695 - gilberto-amelia@uol.com.br

[2] State University of Campinas - Departament of Mechanical Design - PO box 6122, Campinas – SP – Brasil, Zip Code: 13083-970 - robson@fem.unicamp.br

Abstract: Localized faults and transverse cracks are common faults in rotating shafts. The present paper presents the formulation of the damage in a shaft, taking into account that the damage introduces changes in the shaft deformation energy and, hence, changes in the stiffness matrix at the element in which the damage is located. The methodology of fault diagnosis in a flexible rotor with damage supported by active magnetic bearings, provided with an active control system excited by unbalance and white noise is applied. The diagnostic uses correlations functions based on the Ljapunov matrix formulation, and an artificial neural network. The procedure is convenient because it uses only a limited number of easily measurable state variables, computing the correlation between the output variables. It is possible to derive specific relations involving the physical parameters of the system and the correlation matrices of the measured variables. An artificial neural network is used to map the correlations involving variables which are difficult to measure. The proposed fault diagnosis method can detect the faults and find their location in the system.

Keywords: Fault Diagnosis, Magnetic Bearings, Rotor Dynamics, Neural Networks

INTRODUCTION

With recent advances in materials, various kinds, such as the heat resisting alloys and composites, which possess a high strength to weight ratio are increasingly used in high-speed rotating machinery in order to achieve higher levels of availability. However, these materials are vulnerable to damage due to the presence of cracks or moisture absorption. A deterioration of mechanical properties of such materials may occur reducing the fatigue life, the main cause of failure of rotating machinery, Chen et. al (1991).

Localized faults and transverse cracks are common faults in rotating shafts. Under the own weight of the rotor, a crack will open and close once per revolution; this periodic closing and opening is called "breathing". The fault diagnosis can avoid destructive accidents. Many papers deal with mechanical fault diagnosis, only a few include some kind of active control.

Such as the papers by Gash (1993) and Nelson and Nataraj (1986), deal with the dynamics of faults in rotors, especially transverse cracks. Darpe et al. (2004) studied the coupling between longitudinal and torsional vibrations for rotating cracked shafts. The present paper presents the formulation of the damage in a shaft, taking into account that the damage introduces changes in the shaft deformation energy and, hence, changes in the stiffness matrix at the element in which the damage is located, as developed by Chen et. al (1991) and Simões and Steffen (2002).

Using AMB's, Zhu et al. (2003) studied the dynamic characteristics of a cracked rotor; Anton and Ulbrich (1985) investigated a rotor with asymmetrical stiffness and damping properties; Sinha et al. (1993) studied the sensor faults in an electromagnetic suspension system; and Nordmann and Aenis (2002) applied model-based fault detection in a pump with AMB's.

Chiarello and Pederiva (1999) proposed an approach to face of fault detection in stationary dynamic system, the relations between correlation functions and physical parameters are used. Eduardo and Pederiva (2004) expand the proposed formulation introducing the relationship between the Ljapunov matrix and an Artificial Neural Network (ANN) to detect changes in the system; in this methodology it is not necessary to know the parameter values -- it is sufficient to know the model structure. The present work expands this formulation for the case of a more complex mechanical system with damage supported by an Active Magnetic Bearing (AMB), including the action of a closed loop control.

General system configuration

AMB's have a number of interesting characteristics that represent advantages over conventional bearings. They work without any contact or lubrication, and display high dynamical performance, allowing their use as active damping actuators in vibration control. Have been successfully applied in turbomachinery, centrifuges, pumps, and high-

precision machine tools, Brunet (1988). It possesses potential applications in micro-technique such as video heads, medical instruments, hard disk drives, and optical scanners, Schweitzer (2002).

A system having this feature, integrated with fault diagnosis, prognosis and correction systems, constitutes the so-called "Smart Machine Technology".

The rotor system under study is a flexible shaft with four identical discs. The discs at each end are supported by AMB's. The motor acts on one of the intermediate discs, and the rotation sensor is positioned on the other.

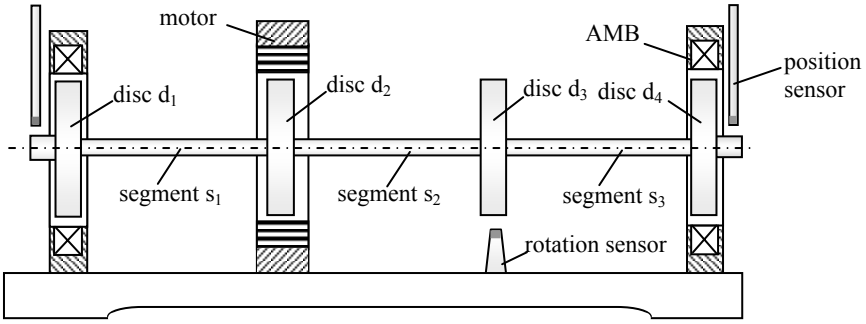

Figure 1 – General system configuration

The closed loop control of the rotor bearing system is essential for stable operation; Fig. 2 shows a basic block diagram of the entire system.

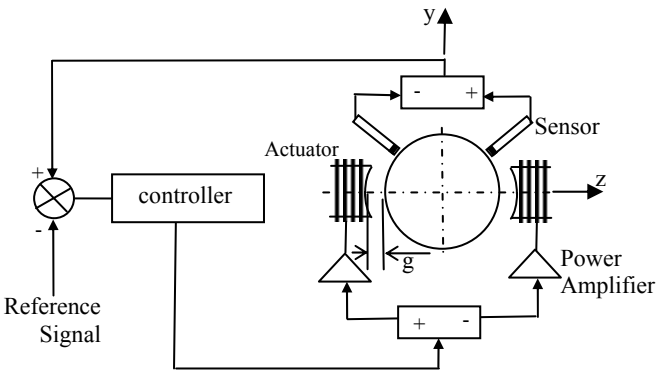

Figure 2 – Closed-loop system-block diagram (z direction)

The position of the rotor is determined by the sensor. The controller receives this information compute and sends a tension signal to the power amplifier. The power amplifier sends a proportional current signal for the actuators. The actuator transforms this signal into magnetic force.

MATHEMATICAL MODEL

AMB model

The relationships between the magnetic force and applied bias currents can be found by:

$$f_m = -km.\left(\frac{i}{g}\right)^2 \tag{1}$$

Where g is the air gap, i is the current in the coils in the z direction, and k_m is a constant that depends of air permeability, number of the windings, and flux cross-sectional area in the air gap. For the radial AMB with two opposite pairs of symmetrical electromagnetic poles, linearizing the magnetic forces, the stiffness elements can be expressed by Alves et. al (1996):

$$km_z = \frac{4.km.i_b{}^2}{g^3} \qquad \text{and} \qquad km_i = \frac{4.Km.i_b}{g^2} \tag{2}$$

$$fz = km_z.z(t) - km_i.i_c(t) \tag{3}$$

Where fz is the the magnetic force in the z direction, i_c is the control current, km_z is the displacement stiffness element of the magnetic bearing, and km_i is the current stiffness element of the magnetic bearing in the z direction. The constants km_z and km_i depend on the chosen design point of the magnetic bearing (bias current i_b and air gap g).

Controller Model

The transfer function of the SISO controller (single in - single out) designed for the 6th order is expressed as:

$$G(s) = \frac{c_5.S^5 + c_4.S^4 + c_3.S^3 + c_2.S^2 + c_1.S + c_0}{S^6 + a_5.S^5 + a_4.S^4 + a_3.S^3 + a_2.S^2 + a_1.S + a_0} \tag{4}$$

The state space equation of the controller for magnetic forces and displacements can be written as:

$$\dot{x}_c(t) = A_c.x_c(t) + B_c.y_c(t) \quad \text{and} \quad f_m = C_c.x_c(t) \tag{5}$$

A_c is the system matrix, x_c is the state vector, B_c is the input matrix, y_c is the output of the mechanical system with sensor gain k_s and C_c is the output matrix of the controller. The matrices have the following structures:

$$A_c = \begin{bmatrix} A_{y1} & 0_{6x6} & 0_{6x6} & 0_{6x6} \\ 0_{6x6} & A_{y4} & 0_{6x6} & 0_{6x6} \\ 0_{6x6} & 0_{6x6} & A_{z1} & 0_{6x6} \\ 0_{6x6} & 0_{6x6} & 0_{6x6} & A_{z4} \end{bmatrix}_{24x24} \qquad x_c = \begin{bmatrix} xc_{y1_{6x1}} & xc_{y4_{6x1}} & xc_{z1_{6x1}} & xc_{z4_{6x1}} \end{bmatrix}^T_{24x1} \tag{6}$$

Where:

$$B_c = \begin{bmatrix} B_{y1} & 0_{6\times1} & 0_{6\times1} & 0_{6\times1} \\ 0_{6\times1} & B_{y4} & 0_{6\times1} & 0_{6\times1} \\ 0_{6\times1} & 0_{6\times1} & B_{z1} & 0_{6\times1} \\ 0_{6\times1} & 0_{6\times1} & 0_{6\times1} & B_{z4} \end{bmatrix}_{24x4} \qquad C_c = \begin{bmatrix} C_{y1} & 0_{1x6} & 0_{1x6} & 0_{1x6} \\ 0_{1x6} & C_{y4} & 0_{1x6} & 0_{1x6} \\ 0_{1x6} & 0_{1x6} & C_{z1} & 0_{1x6} \\ 0_{1x6} & 0_{1x6} & 0_{1x6} & C_{z4} \end{bmatrix}_{8x24} \tag{7}$$

$$B_{yi} = \begin{bmatrix} 1 \\ 0_{5x1} \end{bmatrix}_{6x1} .ks_{yi} \quad \text{and} \quad C_{yi} = \begin{bmatrix} c_0 & c_1 & \dots & c_5 \end{bmatrix}_{6x1} .Km_{yi}.kp_{yi} \tag{8}$$

The matrices: A_{y1}, A_{y4}, A_{z1}, A_{z4} and C_{y1}, C_{y4}, C_{z1}, C_{z4} are the terms of the system and output matrix respectively, for each controller axe (y_1, y_4, z_1, and z_4); ks_{yi}, km_{yi} and kp_{yi} are the sensor, bearing, and power amplifier gains for each controller axe, respectively.

Rotor model

Figure 3 presents the mechanical system. In this modelling the finite element method is used, containing 5 shaft elements, L_1 to L_5 and 4 rigid discs, d_1 to d_4. The 6 nodes are also represented in the Fig. 3.

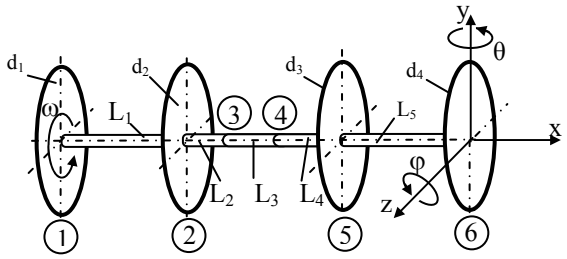

Figure 3 - Mechanical model

The mechanical system may be represented by a differential equation as follows:

$$M.\ddot{\xi} + G.\dot{\xi} + K.\xi = f(t) \tag{9}$$

Where matrix M includes the influence of the second rotatory inertia of the shaft, mass and diametral moments of the disc. Matrix G contains the damping due to the air resistance and gyroscopic effect; matrix K is the stiffness matrix of the shaft; and $f(t)$ are the external forces: white noise, unbalance forces and feedback control forces produced by the magnetic bearing.

The rotation speed of the rotor is ω. Neglecting axial displacements which will be very small, the shaft has the motion described by displacements $y(t)$ and $z(t)$, and rotations $\theta(t)$ and $\varphi(t)$ around the y and z axis respectively. Vector $\xi(t)$ represents system displacements and rotations.

$$\xi(t) = [y_1 \quad z_1 \quad \varphi_1 \quad \theta_1 \quad y_2 \quad z_2 \quad \varphi_2 \quad \theta_2 \quad y_3 \quad z_3 \quad \varphi_3 \quad \theta_3 \quad y_4 \quad z_4 \quad \varphi_4 \quad \theta_4 \quad y_5 \quad z_5 \quad \varphi_5 \quad \theta_5 \quad y_6 \quad z_6 \quad \varphi_6 \quad \theta_6]^T \tag{10}$$

The state space equation of the mechanical system can be written as:

$$\dot{x}_m(t) = A_m.x_m(t) + B_m.f(t), \quad \text{and} \qquad y_m(t) = C_m.x_m \tag{11}$$

$$A_m = \begin{bmatrix} 0_{24x24} & I_{24x24} \\ -M^{-1}.K & -M^{-1}.G \end{bmatrix}_{48x48}, B_m = \begin{bmatrix} 0_{24x8} \\ -M^{-1} \end{bmatrix}_{48x8}, C_m = \begin{bmatrix} I & 0 \end{bmatrix}_{4x48}, \text{and } x_m(t) = \begin{bmatrix} \xi(t) \\ \dot{\xi}(t) \end{bmatrix}_{48x1} \tag{12}$$

The square matrix A_m is called the system matrix; B_m is the input matrix, C_m is the output matrix; and y_m is the vector composed of the measured variables. $x_m(t)$ is the state vector of the mechanical system. The dots indicate differentiations with respect to time.

Mechanical fault model

The mechanical fault under study is modelled by the finite element method as proposed by Simões and Steffen (2002), and Chen et al. (1991). The damage can locate in the portion of the shaft (L_1, L_2, L_3, L_4 or L_5), as shown in Fig. 3. In this region the deterioration per unit length is assumed to be uniform and distributed in such a manner as not to cause a shift in the action line of the resultant force. The coordinates of the region with damage are the same as in Fig 3. The stiffness matrix of the shaft element with damage is:

$$K_d = a_k \cdot \begin{bmatrix} 12 & -12 & -6L_d & -6L_d & 0 & 0 & 0 & 0 \\ & 12 & 6L_d & 6L_d & 0 & 0 & 0 & 0 \\ & & (4+a_d)L_d^2 & (2-a_d)L_d^2 & 0 & 0 & 0 & 0 \\ & & & (4+a_d)L_d^2 & 0 & 0 & 0 & 0 \\ & & & & 12 & -12 & 6L_d & 6L_d \\ & & & & & 12 & -6L_d & -6L_d \\ & & \textit{symetry} & & & & (4+a_d)L_d^2 & (2-a_d)L_d^2 \\ & & & & & & & (4+a_d)L_d^2 \end{bmatrix} \tag{13}$$

$$a_k = \frac{EK_b}{(1+a_d)L_d^3}, \qquad a_d = \frac{12.E.k_b}{G.k_s.L_d^2}, \qquad k_b = \xi_b.I_s, \qquad \text{and} \qquad k_s = \xi_s.S_s \tag{14}$$

Where S_s are the cross-section area and I_s inertia moment of the area, L_d is the damage length, E and G are Young's modulus and shear modulus respectively, k_s represents the loss in cross-section area of the shaft, and k_b the inertia loss. ξ_b and ξ_s are factors representing the magnitude of the losses. Matrix K_d is inserted into the stiffness matrix Eq. (9) on shaft elements L_1, L_2, L_3, L_4 or L_5 when a mechanical fault is simulated.

Complete closed loop system

The state space representation of the final model is obtained from Eq. (5) and (11) and can be written as:

$$\dot{x}_f(t) = A_f.x_f(t) + B_f.f_d(t) \tag{15}$$

where:
$$A_f = \begin{bmatrix} A_m & B_mC_c \\ B_cC_m & A_c \end{bmatrix}_{80x80}, \qquad B_f = \begin{bmatrix} B_m \\ 0_{24x8} \end{bmatrix}_{80x8}, \qquad \text{and } x_f = \begin{bmatrix} x_m \\ x_c \end{bmatrix}_{80x1} \tag{16}$$

A_f is the complete system matrix, B_f is the input matrix, f_d are the external unbalance forces and white noise perturbations, and x_f is the state vector of the complete system in closed loop.

CORRELATION FUNCTIONS AND COMPATIBILITY EQUATIONS

For the development of the fault detection procedure based on the correlation equations, a model simpler than the previous one was chosen, with 4 rigid discs and 3 massless shaft elements. The mechanical model has 16 degrees of freedom (DOF), showed in the Fig. 4.

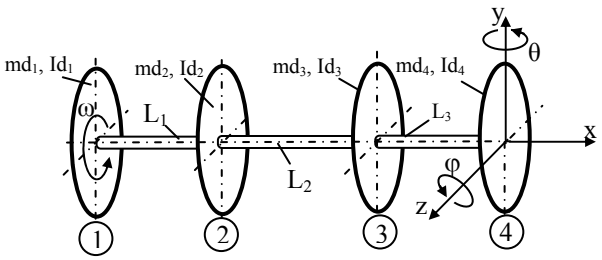

Figure 4 – Mechanical model with 16 DOF

Vector $\xi^*(t)$ represents the displacements and rotations of the system:

$$\xi^*(t) = [y_1 \quad z_1 \quad \varphi_1 \quad \theta_1 \quad y_2 \quad z_2 \quad \varphi_2 \quad \theta_2 \quad y_3 \quad z_3 \quad \varphi_3 \quad \theta_3 \quad y_4 \quad z_4 \quad \varphi_4 \quad \theta_4]^T \tag{17}$$

The complete system including the controller is a 56th-order system, and its state space equation is:

$$\dot{x}^*_f(t) = A^*_f . x^*_f(t) + B^*_f . f_d(t) \tag{18}$$

$$A^*_f = \begin{bmatrix} A^*_m & B^*_m C_c \\ B_c C^*_m & A_c \end{bmatrix}_{56x56}, \qquad B^*_f = \begin{bmatrix} B^*_f \\ 0_{24x8} \end{bmatrix}_{56x8}, \qquad \text{and} \qquad x^*_f = \begin{bmatrix} x^*_m \\ x_c \end{bmatrix}_{56x1} \tag{19}$$

A^*_f, B^*_f and x^*_f are the complete system matrix, input matrix and state vector of the complete new system in closed loop.

The correlation matrix between the states of Eq. (18) $Rx^*_f x^*_f(\tau_i)$ is defined by:

$$Rx^*_f x^*_f(\tau_i) = \varepsilon\left\{ x^*_f(t) . x^{*T}_f(t+\tau_i) \right\} \tag{20}$$

where τ_i represents the time lag.

Evaluating Eq. (20) with the solution of Eq. (18), the following relationship is obtained for a stationary condition, according to Chiarello and Pederiva (1999):

$$A^*_{f\,56x56} . Rx^*_f x^*_{f\,56x56} + Rx^*_f x^*_{f\,56x56} . A^{*T}_{f\,56x56} + B^*_{f\,56x8} . Rn_f x^*_{f\,8x56} + Rx^*_f n_{f\,56x8} . B^{*T}_{f\,8x56} = 0 \tag{21}$$

Equation (21) is called Ljapunov Matrix Equation, and is used to develop the method of fault detection in the present work. Correlation matrices are defined by:

$$Rx^*_f x^*_f = \begin{bmatrix} Rx^*_m x^*_m & Rx^*_m x_c \\ Rx_c x^*_m & Rx_c x_c \end{bmatrix}, \qquad Rn_f x^*_f = \begin{bmatrix} Rx_n x^*_m & Rx_n x_c \end{bmatrix} \qquad \text{and} \qquad Rx^*_f n_f = \begin{bmatrix} Rx^*_m x_n \\ Rx_c x_n \end{bmatrix} \tag{22}$$

Where $Rx^*_m x^*_m$ is the correlation matrix between mechanical states, $Rx^*_m x_c$ between mechanical states and controller states, $Rx_c x^*_m$ correlations between states of the controller and mechanical, $Rx_c x_c$ between controller states, $Rx_n x^*_m$ correlations between unbalance and mechanical states, $Rx_n x_c$ unbalance and controller states, $Rx^*_m x_n$ mechanical and unbalance and $Rx_c x_n$ correlations between controller and unbalance states. Equation (21) contains the relationships involving the correlation functions between system outputs and the physical parameters of differential Eq. (18). These relationships represent the basis for the procedure employed in the current work.

Equation (21) was developed by means of algebraic computation software and resulted in 3136 compatibility equations. In order to select the equations that correlate with mechanical fault parameters, a three-steps method was used: (a) find, within the dynamic state matrix Eq. (18), the element that relates to the fault; (b) select the matrix column that relates to measurable states Eq. (22); and (c) with help of the search command of the software, locate the desired equations. The equations selected for the proposed mechanical faults are:

$$\begin{aligned} &k_{11} . Ry_1 y_1 + k_{12} . Ry_2 y_1 + k_{16} . R\varphi_2 y_1 + R\dot{y}_1 \dot{y}_1 + b_1 . Ry_{1n} y_1 + b_1 . c_{y11} Ry_{11c} y_1 + b_1 . c_{y12} Ry_{12c} y_1 \\ &+ b_1 . c_{y13} Ry_{13c} y_1 + b_1 . c_{y14} Ry_{14c} y_1 + b_1 . c_{y15} Ry_{15c} y_1 + b_1 . c_{y16} Ry_{16c} y_1 + c_{11} R\dot{y}_1 y_1 = 0 \end{aligned} \tag{23}$$

$$k_{21} . Ry_1 y_2 + k_{22} . Ry_2 y_2 + k_{23} . Ry_3 y_2 + k_{25} . R\varphi_1 y_1 + k_{27} . R\varphi_3 y_2 + R\dot{y}_2 \dot{y}_2 + b_2 . Ry_{2n} y_2 + c_{22} R\dot{y}_2 y_2 = 0 \tag{24}$$

$$k_{23} . Ry_2 y_3 + k_{33} . Ry_3 y_3 + k_{34} . Ry_4 y_3 + k_{36} . R\varphi_2 y_3 + k_{37} . R\varphi_3 y_3 + R\dot{y}_3 \dot{y}_3 + b_3 . Ry_{3n} y_3 + c_{33} R\dot{y}_3 y_3 = 0 \tag{25}$$

$$\begin{aligned} &k_{43} . Ry_3 y_4 + k_{44} . Ry_4 y_4 + k_{47} . R\varphi_3 y_4 + R\dot{y}_4 \dot{y}_4 + b_4 . Ry_{4n} y_4 + b_4 . c_{y41} Ry_{41c} y_4 + b_4 . c_{y42} Ry_{42c} y_4 \\ &+ b_4 . c_{y43} Ry_{43c} y_4 + b_4 . c_{y44} Ry_{44c} y_4 + b_4 . c_{y45} Ry_{45c} y_4 + b_4 . c_{y46} Ry_{46c} y_4 + c_{44} R\dot{y}_4 y_4 = 0 \end{aligned} \tag{26}$$

The parameters k_{ij}, c_{ij} and b_1, b_2, b_3, b_4 are the terms of the matrices A^*_m and B^*_m, which are part of Eq. (19). Parameters ay_{1i}, ay_{4i}, az_{1i}, az_{4i} and $cy_{ij} = c_{ij} . kp . km$ are the terms of the matrices A_c and C_c, Eq. (6) and (7).

Equations (23) to (26) just a few number of correlations functions can be estimated, because of the measuring restriction condition imposed. This method for fault diagnosis in stationary rotor systems uses the correlation analysis and artificial neural network (ANN) with a multi-layer perceptron to map the correlation functions involving variables that cannot be directly estimated, showed in Fig. 5.

NUMERICAL RESULTS AND ANALYSIS

The parameters of the system without faults are listed in Tab. (1) and (2), where each AMB axis is denoted by subscripts (y_1, y_4, z_1 and z_4).

Table 1- Mechanical parameter value

Parameter	*value*	*unit*
md_1,md_2,md_3,md_4	8.80×10^{-2}	kg
Id_1,Id_2,Id_3,Id_4	3.10×10^{-5}	Kg.m^2
Ip_1,Ip_2,Ip_3,Ip_4	6.02×10^{-5}	Kg.m^2
I_s	5.10×10^{-11}	Kg.m^2
A_s	1.57×10^{-5}	m^2
ω	315	rad/s

Table 2- Bearing parameter value

Parameter	*value*	*unit*
$ks_{y1}=ks_{y4}=ks_{z1}=ks_{z4}$	19000	V/m
$kp_{y1}=kp_{y4}=kp_{z1}=,kp_{z4}$	-0.25	A/V
$km_{y1}=km_{y4}=km_{z1}=km_{z4}$	8	N/A
$k_{y1}=k_{y4}=k_{z1}=k_{z4}$	-2450	N/m
$i_{by1}=i_{by4}=i_{bz1}=i_{bz4}$	0.307	A
g	1	mm

The compatibility Eq. (23) to (26) has different dependences on the parameters. Equations (23) and (26) are sensitive to shaft and bearing stiffness at nodes (1) and (4). Equations (24) and (25) are only sensitive to shaft stiffness associated to nodes (2) and (3). These dependences are very useful not only to determine parameter variations but also to locate where a failure is present. It is not necessary to know the parameter value

ANN's configuration

The equation terms containing correlation functions of variables that cannot be directly measured are modelled by the ANN. To detect the faults each of the Eq. (23) to (26) the inputs and outputs are listed in Tab. 3.

Table 3: ANN's - Inputs and Outputs

Equation.	*State*	*Node*	*Inputs*	*Output*	*Network.*
23	y_1	1	$\Rightarrow Ry_2y_1, R\dot{y}_1R\dot{y}1, Ry_{11c}y_1, Ry_{12c}y_1, Ry_{13c}y_1$	$\Rightarrow Ry_1y_1$	$\Rightarrow$ A1
24	y_2	2	$\Rightarrow Ry_1y_2, Ry_3y_2, R\dot{y}_2\dot{y}_2, R\dot{y}_2y_2$	$\Rightarrow Ry_2y_2$	$\Rightarrow$ A2
25	y_3	3	$\Rightarrow Ry_2y_3, Ry_4y_3, R\dot{y}_3\dot{y}_3, R\dot{y}_3y_3$	$\Rightarrow Ry_3y_3$	$\Rightarrow$ A3
26	y_4	4	$\Rightarrow Ry_3y_4, R\dot{y}_4\dot{y}_4, Ry_{41c}y_4, Ry_{42c}y_4, Ry_{43c}y_4$	$\Rightarrow Ry_4y_4$	$\Rightarrow$ A4

The Levenberg-Maquart algorithm was used to train the network. The ANN architecture contains 10 neurons on the first layer and 10 neurons on the second layer, and the unit activation function is sigmoidal. All neurons from one layer are connected to all neurons in the next layer, Fig. 5.

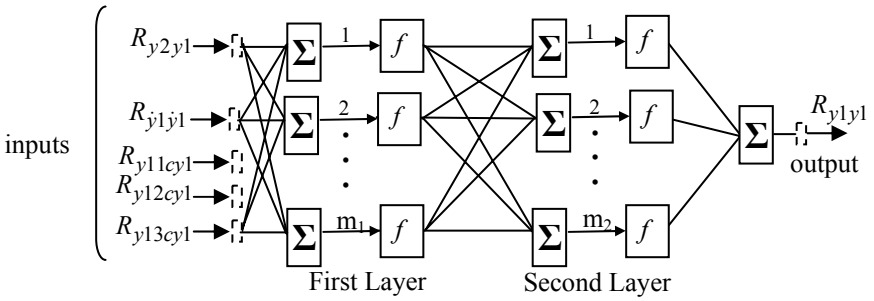

Figure 5 - Multi layer perceptron to map equation 23

Mechanical faults

The comparison between the autocorrelations of the signals without mechanical fault and with mechanical fault was done by computing the MSD indices by the following equation:

$$MSD = \sqrt{\frac{1}{N}\sum_{k=1}^{N}(y_k - \bar{y}_k)^2} \tag{27}$$

where: the network output is y_k and the estimated response is $\bar{y}_k$. N is the number of points.

Figures 6 to 14 show the results for the case of damage in the shaft at segments s_1, s_2 and s_3, considering the parameters of the mechanical faults as follows: $\xi_s = \xi_b = 0.7$ and $L_d = 0.02$ m.

Case 1: Mechanical Fault at Central Shaft Segment- s_2

For this case the disc d_1 is positioned in node (1), the disc d_2 is in node (2), the disc d_3 is in node (5) and disc d_4 is in node (6). The faults were applied to shafts element L_2, L_3 e L_4 respectively, by means of Eq. (13) and (14). The following results were found:

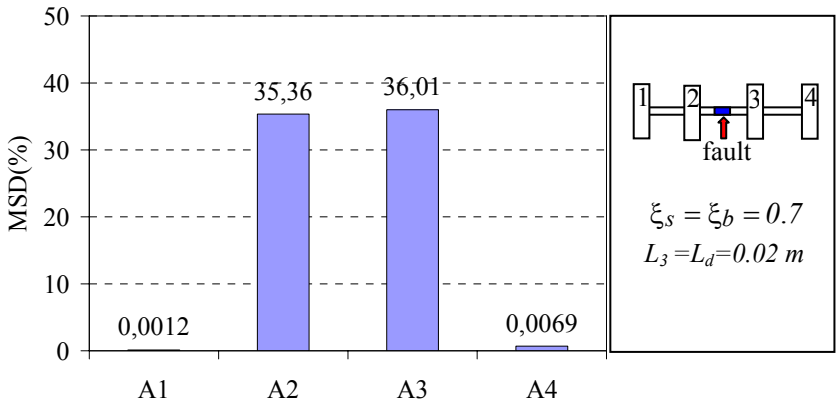

Figure 6 – Mechanical fault – central damage - segment s_2

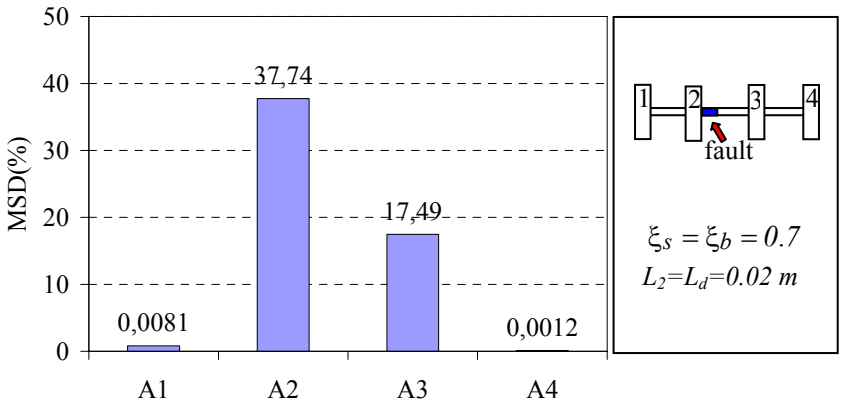

Figure 7 – Mechanical fault - damage near disc d_2 - segment s_2

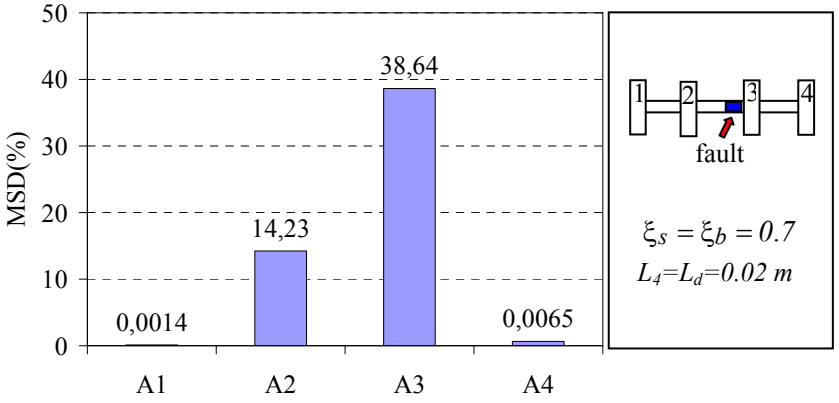

Figure 8 – Mechanical fault – damage near disc d_3 - segment s_2

In Fig. 6, for a central fault at segment s_2, the MSD indicates that the fault is located between the two adjacent nodes (2) and (3). The deviations are equally distributed in networks A2 and A3; in Fig. 7 it was predominant in node (2); and in Fig. 8 in node (3), as expected. It is interesting to notice that only one sensor in central discs already guarantees the detection the fault in this region.

Case 2: Mechanical Fault at Shaft Segment- s_1

For this case disc d_1 is positioned in node (1), disc d_2 at node (4), disc d_3 is in node (5) and disc d_4 is in node (6). The fault applied to shafts element L_1 , L_2 and L_3 respectively, by means of Eq. (13) and (14). The following results were found:

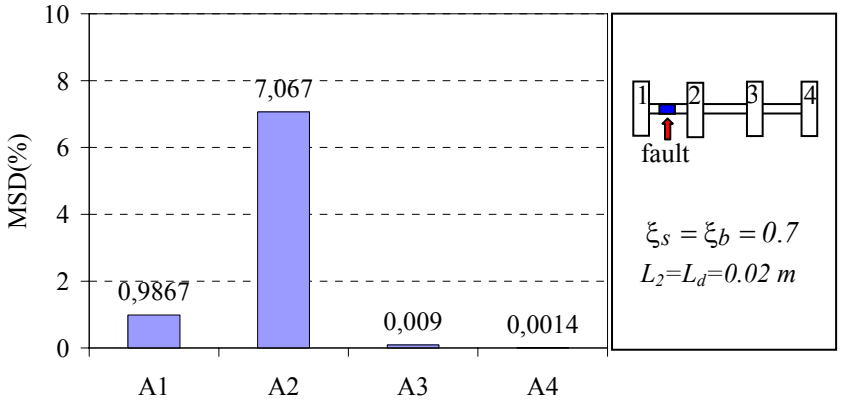

Figure 9 – Mechanical fault - central damage - segment s_1

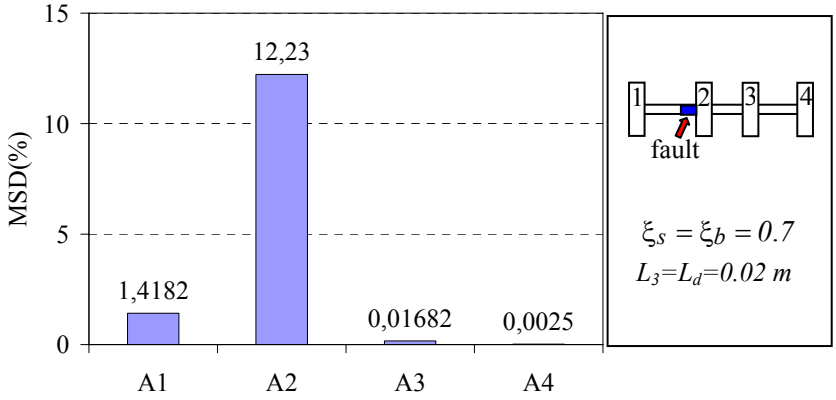

Figure 10 – Mechanical fault - damage near disc d_2 - segment s_1

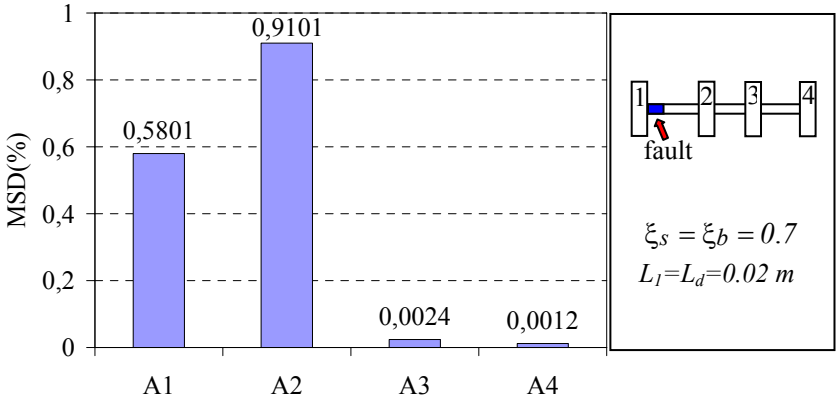

Figure 11 – Mechanical fault - damage near disc d_1- segment s_1

In Fig. 9, for a central fault at segment s_1, the MSD indicates that the fault was predominant in node (2), network A2. However relatively to the network A1 the deviation was not accented. In Fig. 10 it was more predominant in network A2 and small in network A1. In Fig. 11 small deviations in networks A1 and A2 can be seen. These deviations are not significant when compared with other analyzed cases. However, they have shown coherent due to localization to be near of the bearing.

Case 3: Mechanical Fault at Shaft Segment- s_3

For this case disc d_1 is positioned in node (1), disc d_2 is in node (2), disc d_3 is in node (3) and disc d_4 is in node (6). The fault applied to shafts element L_3 , L_4 and L_5 respectively, by means of Eq. (13) and (14). The following results were found:

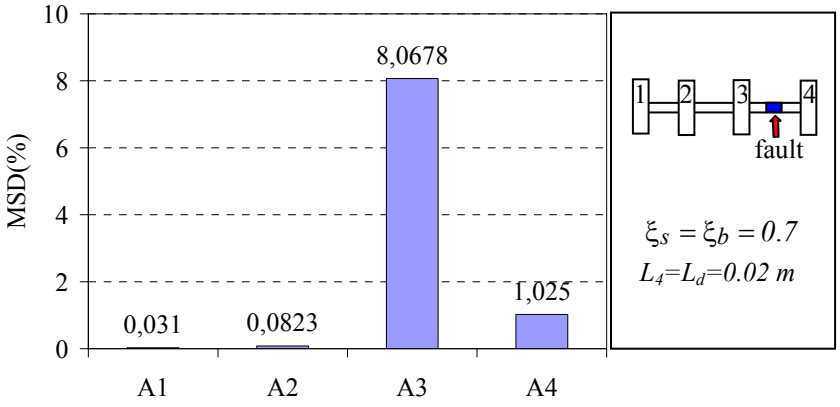

Figure 12 – Mechanical fault – central damage - segment s_3

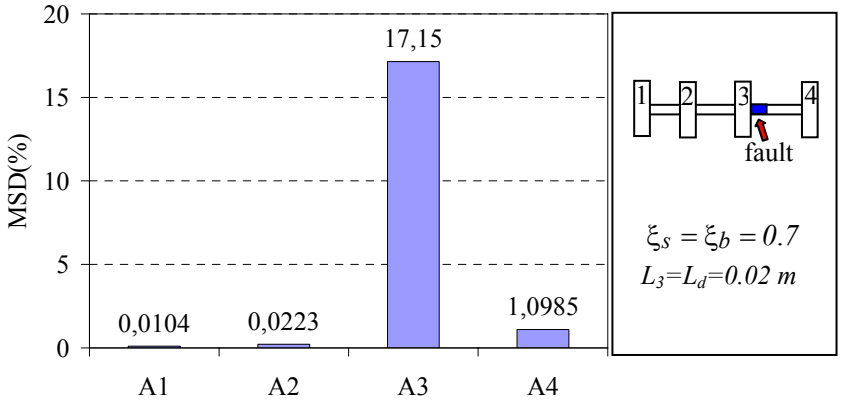

Figure 13 – Mechanical fault – damage near disc d_3 - segment s_3

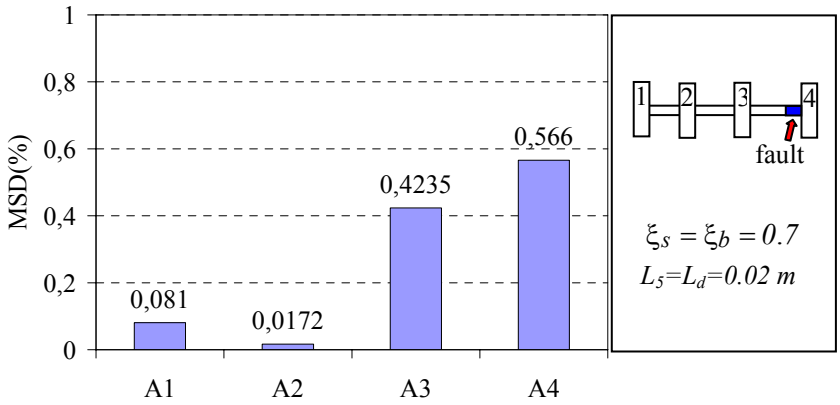

Figure 14 – Mechanical fault – damage near disc d_4 - segment s_3

In Fig. 12, for a central fault the MSD indicates that the fault is located between the two adjacent nodes (3) and (4). It was predominant in node (3) network A3; In Fig. 13 the effect was more predominant in network A3 and small in network A4. The deviations presents in networks A_3 and A_4, Fig. 14, are not significant when compared with other analyzed cases. However, they have shown also coherent due to the fault localization to be near of the bearing.

CONCLUSION

A method of fault monitoring system was developed, by means of the Ljapunov Matrix Equation and an artificial neural network, in a rotor with active magnetic bearing and control system. Although the model used in this study was of a high order, and the limitations of the measured states were severe, very good results were obtained. In this method it is not necessary to know the value of model parameters: the model structure is sufficient

The studied cases of mechanical fault presented satisfactory results. It is possible to detect the mechanical fault and its location within the system. The method presented some limitations for the cases of the fault near to the bearing because the unbalance configuration simulated basically excites the first bending mode and these points to be on the node of the mode.

These are good indications that the proposed approach deserves further study. An experimental set-up has already been built to study the method under practical limitations such as measurement errors, non-linearities, and noise.

REFERENCES

Anton, E.;Ulbrich,H.(1985), "Active Control Vibrations in the Case of Asymmetrical High-Speed Rotors by using Magnetic Bearings"., Journal of Vibration, Acoustics, Stress, and Reliability in Design.Vol. 107, pp. 410–415

Alves, J.S.;Betti,F.;Pierri,P.S.;Porsh,M.C. (1996), "Control System for Active Magnetic Bearing", Proceedings of the Simposio de Automatica Aplicada. São Paulo, Brasil, Sept. 18-20, pp. 135–140.

Brunet, M. (1988), "Practical Application of the Active Magnetic Bearing to Industrial World", Proceedings of the First International Symposium on Magnetic Bearings. Zurich, Swiss, Jun. 6-8, pp.225-244.

Chen, L.W.;Ku,D.M.(1991)," Whirl Speeds and Unbalance Response of a Shaft-Disk System With Flaws", The International Journal of Analytical and Experimental Modal Analysis. Vol. 6, pp. 279–289

Chiarello, A. G.; Pederiva R. (1999), "A study of parameter monitoring in stationary mechanical system", RBCM Journal of the Brazilian Society of Mechanical Sciences, Vol. XXI, No. 1, pp 123-132.

Darpe, A.K.;Gupta,K.(2004), "Coupled Bending, Longitudinal and Torsional Vibrations of a Cracked Rotor", Journal of Sound and Vibration. Vol 269, pp. 33–60

Gash, R. (1993), "A Survey of the Dynamic Behaviour of a Simple Rotating Shaft With a Transverse Crack.", Journal of Sound and Vibration. Vol. 160(2), pp. 313–332

Haykin, S. (1999), "Neural Networks: A Comprehensive Foundation", Prentice Hall, New Jersey, USA

Lalanne, C.;Ferraris,G.(1998) "Rotordynamics Prediction in Engineering: A Comprehensive Foundation", John Wiley and Sons, Chichester, England.

Nelson, H.D.;Nataraj,C.(1986), "The Dynamics of a Rotor System with a Cracked Shaft", Journal of Vibration, Acoustics, Stress, and Reliability in Design. Vol. 108, pp. 189–206

Nordmann, R.;Aenis,M. (2002), "Fault Diagnosis in a Centrifugal Pump using Active Magnetic Bearing.", In Proc Sixth International Conference on Rotor Dynamics. Sydney, Australia, Sept.30- Oct.4, pp.46-55.

Pederiva, R.; Eduardo A.C. (2002), "Parameter Monitoring of a rotor system excited by Stochastic Forces", Proceedings Sixth International Conference on Rotor Dynamics. Sydney, Australia.,Sept. 30- Oct. 4, pp.310-317.

Simões, R.C.;Steffen Jr.,V. (2002), "About the Problem of Fault Identification in Rotating Machinery", In Proc II National Congress of Mechanical Engineering. João Pessoa, Brasil, Aug. 12-16, pp.9-14.

Sinha, P.K.;Zhou,F.B.;Kutiyal,R.S.(1993), "Fault Detection in Electromagnetic Suspension Systems with State Estimation Methods", IEEE Transactions on Magnetics.Vol.29, pp. 2950–2952.

Zhu, C.;Robb, D.A.,Ewins, D.J.(2003), "The Dynamics of a Cracked Rotor with Active Magnetic Bearing", Journal of Sound and Vibration. Vol. 265, pp. 469–487

RESPONSIBILITY NOTICE

The authors are the only responsible for the printed material included in this paper.